



# Economical Adsorbent Developed from Sugarcane Bagasse for Zinc (II) Removal from Wastewater

Melkamu Birhie Genet · Addis Lemessa Jembere · Gedefaw Asmare Tafete 

Received: 22 March 2022 / Accepted: 10 July 2022 / Published online: 20 July 2022  
© The Author(s), under exclusive licence to Springer Nature Switzerland AG 2022

**Abstract** Sugarcane bagasse activated carbon (SBAC) was used as an environmentally friendly adsorbent for the removal of zinc (II) heavy metal from aqueous solutions at neutral pH. Zinc (II) adsorption efficiency was evaluated at different process parameters including adsorbent dosage, contact time, and temperature using general factorial as an experimental design to evaluate the maximum adsorption efficiency. The synthesized SBAC was subjected to advanced characterization techniques that include FTIR, XRD, and TGA/DTA to study the functional groups, crystallinity, and thermal property, respectively. Chemically modified SBAC was able to reduce initial metal concentrations by 82.4%. The optimized process parameters that give maximum removal efficiency were obtained at 40 min, 6 gm, and 60 °C. The experimental data were fitted to Langmuir, Freundlich, and Temkin models. Pseudo-first-order, pseudo-second-order, and intraparticle diffusion models were used to model adsorption kinetics. The experimental data were best fitted to the pseudo-second-order kinetic model with Langmuir isotherm. An important parameter from the isotherm which indicates adsorption capacity

was 426.64 mg/g. The thermodynamic parameters for entropy,  $\Delta S$ , enthalpy,  $\Delta H$ , and the Gibbs free energy,  $\Delta G$ , reveal that the adsorption of zinc (II) by the SBAC is endothermic, thermodynamically feasible, and a spontaneous process.

**Keywords** Activated carbon · Adsorption · Heavy metal · Sugarcane bagasse · Zinc (II)

## 1 Introduction

The paramount discharge of heavy metals into the globe has been increasing continuously due to industrial activities and technological developments, posing a significant threat to the environment and public health because of their toxicity, build-up in the food chain, and persistence in nature (Khalfaoui & Meniai, 2012; Khalfaoui & Meniai, 2012; Mahmoud, 2014; Rengaraj et al., 2001; Wuana & Okieimen, 2011). It is therefore very crucial to remove these nonbiodegradable toxic heavy metals from industrial effluents. Zinc, Cadmium, arsenic, copper, nickel, lead, mercury, iron, and chromium are the major heavy metal contaminants regularly detected in industrial effluents that arise from metal plating, battery manufacture, smelting, mining activities, tanneries, petroleum refining, paint manufacture, pesticides, pigment manufacture, radiator manufacturing, alloy industries printing, and photographic industries (Kadirvelu et al., 2001).

M. B. Genet · A. L. Jembere · G. A. Tafete (✉)  
Faculty of Chemical and Food Engineering, Bahir Dar  
Institute of Technology, Bahir Dar University, Bahir Dar,  
Ethiopia  
e-mail: gedepeng@gmail.com

Zinc is a predominantly used heavy metal in electroplating industries and discharges paramount effluents to the environment. It is very toxic if the amount of zinc intake exceeds 100 mg/day (Senthilkumar et al., 2006). Zinc harmfulness to humans has been found in both acute and chronic forms. Toxicity from chronic ingestion of zinc can result in copper deficiency. Ingestion of this heavy metal bounds from 100 to 150 mg/day affects copper metabolism and causes low copper levels in the body, decreased iron function, red blood cell microcytosis, neutropenia, reduced immune function, and decreased levels of high-density lipoproteins (F. V. Pereira et al., 2010). Ingesting 200–800 mg/day of zinc can cause abdominal pain, nausea, vomiting, and diarrhea. There are other reported effects including lethargy, anemia, and dizziness (F. V. Pereira et al., 2010). To protect freshwater, marine aquatic life, and agricultural water, guidelines for zinc discharging limits have been developed by several nations. For example, the United States Environmental Protection Agency (USEPA) sets up the maximum discharge limits of zinc at 4.2 mg/L for any 1-day value and 2.6 mg/L for the average daily values for four consecutive monitoring days.

Different methods are utilized to expel heavy metals in water and wastewater such as chemical precipitation, ion exchange, reverse osmosis, electro-dialysis, ultrafiltration, and phytoremediation. However, the high cost associated with these methods has urged us to explore cheaper alternatives. Adsorption is found to be the most effective, plentiful, simple operation, versatile and broadly used, and efficient method to treat water and wastewaters containing heavy metals compared to other treatment techniques (Ali & Gupta, 2007; Demirbas, 2008; Gupta & Ali, 2004; Salihi, 2015).

Pereira et al. (F. V. Pereira et al., 2009) studied zinc removal efficiency from electroplating wastewater in batch and continuous mode using modified succinic anhydride sugarcane bagasse and wood sawdust. They found 95% removal efficiency in batch mode at 1.0 g/L adsorbent concentration and 65.7% and 57.8% for continuous mode using sugarcane bagasse and wood sawdust modified, respectively. Other researchers also investigated the removal efficiency of zinc using sand as an adsorbent. The removal efficiency was quite high ranging from 71 to 87% (Aslam, 2004).

Most low-cost adsorbents were prepared from lignocellulosic raw materials that are available in massive amounts that can be byproducts of industrial processes or agricultural wastes (Šćiban et al., 2007; Wan Ngah & Hanafiah, 2008). Sugarcane bagasse is abundantly available as a byproduct in sugarcane mill industries which can be utilized to prepare low-cost adsorbents to treat heavy metals from aqueous industrial effluent due to its high lignin, hemicelluloses, cellulose, and carbon content (Anoop Krishnan & Anirudhan, 2002; Guan et al., 2013; Gupta & Ali, 2000; Hassan & El-Wakil, 2003; Karnitz et al., 2007; Nada & Hassan, 2006; Srivastava et al., 2006). Sugarcane bagasse is a fibrous residue of cane stalks cleared out after pulverizing and extraction of the juice from sugarcane industries. Almost 54 million dry tons of bagasse are produced yearly throughout the globe (Mulinari et al., 2009). On average, sugarcane bagasse contains almost 45–50% moisture, 43–52% fiber, and 2–6% soluble solids. The typical composition of bagasse fiber is around 26.6–54.3% cellulose, 22.3–29.7% hemicellulose, and 14.3–24.45% lignin (Katyal et al., 2003). Making use of sugarcane bagasse including its fly ash remaining from the boiler house is still recognized by the latest research works on the adsorption process for the application of wastewater treatment due to its abundant availability in sugar industries (Jembere & Genet, 2021).

Many biosorbents have been developed and tested for zinc removal from aqueous solutions, for instance, fruit rinds (Yılmaz & Tugrul, 2022), activated palm midrib (Mulana et al., 2018), urban pruning waste (Sia et al., 2022), rice husk ash, and derived hybrid (Jagaba et al., 2020). However, the adsorption capacity of these biosorbents is low (<40 mg/g). It would thus be of interest to find high adsorption capacity biosorbents like SBAC for zinc removal from wastewater. The objective of this study is to investigate the adsorption characteristic of Zn (II) ions from aqueous solutions using sugarcane bagasse activated carbon (SBAC) as low-cost adsorbents. The effect of time, temperature, and adsorbent dosage on metal ions' adsorption onto these adsorbents have been investigated and optimized. Adsorption isotherms, kinetics, mechanism, and thermodynamics of the adsorption process have been studied.

## 2 Materials and Methods

### 2.1 Materials

Sugarcane bagasse (SB) was collected from Wonji Shewa Sugar Factory, Ethiopia. A stock solution of zinc ions was prepared by dissolving the appropriate amount of  $ZnSO_4 \cdot 7H_2O$  in distilled water. The pH of the solutions was adjusted by 0.01 M NaOH or 0.01 M HCl solution. All the reagents used were of analytical grade chemicals (brand of Merck) and obtained from Bahir Dar Institute of Technology, Chemical Engineering Laboratory, Ethiopia.

### 2.2 Preparation of Adsorbent

The bioadsorbent preparation technique is adopted according to the method by Kim et al., (2001), whereby sulfuric acid treatment is followed by carbonization. Because impregnation with sulfuric acid before carbonization appeared to increase the yield and porosity of the activated carbon, the preparation procedure was simple and economical. The SB was repeatedly washed with tap water to remove specks of dust and mud. Then, it was sun-dried and washed again with distilled water to eliminate other remaining impurities. Then, SB was oven-dried at 100 °C for 24 h to de-moisturize. After that, it was pulverized using a disc mill to convert it into a fine powder. The SB powder which passed 0.5-mm sieve size was taken for adsorbent preparation to get a uniform particle size. The SB was then treated with 0.2 M  $H_2SO_4$  for 12 h to remove soluble impurities. Subsequently, it was washed with distilled water to maintain a neutral pH, and then, it was dried again in an oven at 60 °C for 24 h before activation. Finally, it was carbonized using a muffle furnace at 650 °C for 2 h in an inert atmosphere to prepare sugarcane bagasse activated carbon (SBAC), and it was stored in a desiccator for further use.

### 2.3 Proximate Analysis of Sugarcane Bagasse

The proximate analysis of SB was conducted to determine moisture content, volatile matter, ash content, and fixed carbon using standard methods. The sugarcane bagasse moisture content was determined using an oven at a temperature of 105 °C until a steady weight was maintained. The ash content and volatile matter (VM) of the SB sample were determined using a muffle furnace according to standard testing methods. The fixed carbon (FC) of sugarcane bagasse can be calculated using Eq. (1). Triplicate experimental runs were performed for all analyses, and the average values were taken for each parameter. Table 1 shows the ASTM standards used for proximate analysis.

$$FC(\%) = 100 - \%VM - \%Ash \quad (1)$$

### 2.4 Adsorbent Characterization

#### 2.4.1 FTIR Analysis

FTIR characterization was carried out to distinguish the main functional groups present in the SBAC adsorbent responsible for surface adhesion. Two milligrams of SBAC adsorbent was mixed thoroughly with 200 mg of potassium bromide (KBr) and homogenized in an agate mortar. Then, it was placed in the sample compartment of infrared Fourier transform spectroscopy (FT/IR-6600 type A) found in Bahir Dar University, Chemical Engineering Department, and the measurement was scanned in the range between 400 and 4000  $cm^{-1}$  at a resolution rate of 4  $cm^{-1}$ .

#### 2.4.2 XRD

The crystallinity analysis of SBAC adsorbent was conducted using the X-ray diffraction method.

**Table 1** ASTM standards used for proximate analysis

Properties	Test method
Moisture content	(ASTM E 1756, 2015)
Ash content	(ASTM E 1755, 2007)
Volatile matter	(ASTM E 872, 2013)
Fixed carbon content	(ASTM E 1755, 2007) and (ASTM E 872, 2013)

The characterization was performed at Addis Ababa University, Department of Chemistry, using X-ray diffractometer SHIMADZU-7000 Corporation (Tokyo, Japan) using copper radiation  $\text{CuK}\alpha$  ( $\lambda = 0.154 \text{ nm}$ ), at an accelerating voltage of 40 kV and working current of 30 mA. All patterns in the range of  $2\theta$  from  $10^\circ$  to  $80^\circ$  were recorded. Each sample having a mass of 0.25 gm was pressed under 50 MPa to form pellets with an average diameter of 25 mm. The final result was presented in terms of  $2\theta$  (degrees) vs. intensity (count).

### 2.4.3 TGA and DTA Analysis

Thermogravimetric analysis was performed using SDT Q600 TA Instrument in 90- $\mu\text{L}$  alumina crucibles which are found in Bahir Dar University, Chemical Engineering Department. Samples were heated from 25 to 800  $^\circ\text{C}$ , in  $\text{N}_2$  atmosphere, at a heating rate of 10  $^\circ\text{C}/\text{min}$ , in which samples of nearly 5.0 to 6.0 mg were used. Thermogravimetric curves were registered between 25 and 800  $^\circ\text{C}$ .

## 2.5 Batch Adsorption Studies

Adsorption studies were performed based on a batch operation to investigate the influence of different factors on the adsorption of Zn (II) ions onto the SBAC surface. For adsorption studies, 250-mL conical flasks' capacity was used that contain 75 mL of solution. The parameters investigated in the experiment were contact time (20, 40, and 60 min), temperature (30, 45, and 60  $^\circ\text{C}$ ), and adsorbent dosage (2, 4, and 6 g). All experiments were carried out at a fixed pH of 7 and an initial concentration of 2.1 g/L. The obtained data were employed to develop equilibrium and kinetic models. The removal percentage of zinc (II) was calculated for each run by Eq. (2):

$$R(\%) = \frac{C_0 - C_t}{C_0} * 100 \quad (2)$$

where  $C_0$  is the initial concentration (mg/L) and  $C_t$  is the final concentration at time  $t$  of the zinc (II) ion in the solution.

The adsorption capability of an adsorbent, which is obtained from the mass balance on the sorbate in a system with solution volume ( $V$ ), was regularly used to determine the experimental adsorption isotherms.

Under experimental conditions, the adsorption capacity of all adsorbents was calculated for each concentration of equilibrium zinc (II) ions using Eq. (3):

$$q_e = \frac{(C_0 - C_e) * V}{m} \quad (3)$$

where  $q_e$  (mg  $\text{g}^{-1}$ ) is the amount of Zn (II) ions adsorbed at equilibrium,  $C_0$  (mg  $\text{L}^{-1}$ ) is the initial concentration of Zn (II) ions,  $C_e$  (mg  $\text{L}^{-1}$ ) is the concentration of Zn (II) ions in solution at equilibrium,  $V$  (L) is the volume of Zn (II) ions, and  $m$  (g) is the mass of the adsorbent.

### 2.5.1 Adsorption Equilibrium Isotherm

The maximum or ultimate adsorption capacity was determined using an adsorption isotherm. There exist six types of adsorption isotherms, and the important design parameters are calculated from the batch adsorption experiments. The most commonly utilized models include Langmuir, Freundlich, and Temkin isotherms.

**Langmuir adsorption isotherm:** The Langmuir adsorption isotherm depicts the surface as homogeneous assuming that all the adsorption sites have equal adsorbate affinity and that adsorption at one site does not influence adsorption at an adjacent site (Armbruster & Austin, 1938). It is valid for monolayer adsorption onto the adsorbent (Armbruster & Austin, 1938). The nonlinear and linear form of the Langmuir equation is represented in Eqs. (4) and (5), respectively:

$$q_e = \frac{q_{max}bc_e}{1 + bc_e} \quad (4)$$

$$\frac{C_e}{q_e} = \frac{1}{q_{max}b} + \frac{C_e}{q_{max}} \quad (5)$$

where  $q_e$  is the quantity of solute adsorbed in line with the unit weight of adsorbent (mg/g),  $C_e$  is the equilibrium concentration of solute inside the bulk solution (mg/L),  $q_{max}$  is the monolayer adsorption capability (mg/g), and  $b$  (L/mg) is the Langmuir consistent associated with the adsorption capability and strength of adsorption, respectively.

**Freundlich isotherm:** This isotherm developed by Freundlich (Freundlich, 1906) portrays the

equilibrium on heterogeneous surfaces and does not assume monolayer capacity. The nonlinear and linear form of the Freundlich equation is presented in Eqs. (6) and (7), respectively:

$$q_e = K_F C_e^{\frac{1}{n}} \quad (6)$$

$$\log q_e = \log K_F + \frac{1}{n} \log C_e \quad (7)$$

where  $q_e$  is the amount of solute adsorbed per unit weight of adsorbent (mg/g),  $C_e$  is the equilibrium concentration of solute in the bulk solution (mg/L), and  $K_F$  is a constant that describes the relative adsorption capacity of the adsorbent (mg/g) and the constant  $1/n$  shows the intensity of the adsorption.

**Temkin adsorption isotherm model:** Temkin and Pyzhev (Temkin, M. J., 1940) describe the interaction between adsorbing species and adsorbents among adsorption isotherms, and this equation can be indicated in linear form in Eq. (8):

$$q_e = B \ln K_T + B \ln C_e \quad (8)$$

where  $K_T$  is the Temkin equilibrium binding constant (L/mg) and  $B = RT/b$  is concerning the heat of adsorption (J/mol).

### 3 Results and Discussion

#### 3.1 Proximate Analysis

The proximate analysis determines the gross biomass components in terms of fixed carbon content, volatile matter, ash content, and moisture content of the SB sample. Table 2 shows the proximate analysis of SB. The moisture content of the SB used in this study was 10.3% on a dry mass basis, and the value of this result agrees with the moisture contents of SB

reported by different works of literature as shown in Table 2. Low moisture content shows that the adsorption of moisture by using the SB samples was small, and the moisture content has no substantial effect on adsorptive power unless it increases the weight and hinders the porous nature of adsorbents (Jawad et al., 2017). The ash content of the SB was found as 4.56% on a dry mass basis, and this value is similar to the ash content reported by various works of literature as indicated in Table 2. The good adsorbent has low ash content; otherwise, it can lead to increase hydrophilicity and can have catalytic effects, causing the restructuring process during the regeneration of used adsorbents (Ahmad et al., 2013). The volatile matter contents were found to be 74.6% by dry mass basis, and these values are very close to those previously reported for bagasse as depicted in Table 2. During the activation step, natural molecules present in adsorbents liberate as volatile matter leaving behind a rigid carbon skeleton in the form of aromatic sheets and strips (Bello et al., 2017; Jawad et al., 2019), and additionally, significant quantities of mineral matter, carbonates, oxides, and sulfides were removed (Ahmad et al., 2013). The fixed carbon contents are found to be 14.1% on a dry basis, and different researchers for SB as shown in Table 2 report similar values. This may be attributed to the greater competition between activators and carbon as well as other elements existing in the adsorbent to discharge more unstable components with associated improvement in the textural characteristics and carbon burn-off (Mopoung et al., 2015).

#### 3.2 FTIR Analysis

Participating functional groups in SBAC are determined by FTIR spectroscopy as shown in Fig. 1. The major peaks found in the spectra were at wave numbers 477, 600, 715, 1122, 1606, 1706, and

**Table 2** Proximate analysis of SB

Contents	This study	Literature	Reference
Moisture	10.3	8–14	(Katyal et al., 2003; Mesa-Perez et al., 2005; Tsai et al., 2006)
Ash	4.56	5–6	(Qian et al., 2020; Tsai et al., 2006)
Volatile matter	74.6	73–84	(Katyal et al., 2003; Tsai et al., 2006; J. J. Lu & Chen, 2015; Garca-Pèrez et al., 2002)
Fixed carbon	14.1	12–18	(Katyal et al., 2003; Qian et al., 2020; J. J. Lu & Chen, 2015; Garca-Pèrez et al., 2002; Channiwala & Parikh, 2002)

3480. The broad and strong absorption band at 3100–3600  $\text{cm}^{-1}$  demonstrated stretching hydroxyl (–OH) or amine (–NH) groups which are intermolecular-bonded primary amine and alcohols classes. The band at 1706  $\text{cm}^{-1}$  attributed to stretching carbonyl (–C=O) groups (carboxylic acid, acetate groups, ketone, aldehyde), and the 1606  $\text{cm}^{-1}$  band belongs to (C=C) stretching vibration in conjugated alkenes. The peak at 1122  $\text{cm}^{-1}$  indicates the presence of a functional group (C–O stretching) which is responsible for the group of aliphatic ether and secondary alcohols. The 716 and 600  $\text{cm}^{-1}$  peaks showed the presence of C–H bending aromatics and C–Br or C–I halo compounds (Hu et al., 2011; Petrov et al., 2000; Rajbhandari et al., 2013). Silica which is the main component of sugarcane bagasse ash (Dlapa et al., 2013; Govindarajan & Jayalakshmi, 2011) represented by peaks located between 700 and 1200  $\text{cm}^{-1}$  in the FTIR spectra (Capeletti & Zimnoch, 2016). Thus, the observation from Fig. 1 shows that the ash content of the SBAC samples is very low. This is because the SBAC has low inorganic and volatile constituents which were achieved during activation. The functional groups found in the SBAC especially hydroxyl (–OH) and carboxyl (R–COOH) groups can bind heavy metals by donation of an electron pair from these groups to form complexes with metal ions in an aqueous solution (Kılıç et al., 2014; Maia et al., 2021; Phuengphai et al., 2021; Safari et al., 2019; Yılmaz & Tugrul, 2022). The FTIR result supports that the

use of SBAC biosorbent is appropriate for heavy metal adsorption from an aqueous solution.

### 3.3 X-Ray Diffraction

The X-ray diffraction pattern of SBAC presented in Fig. 2 reveals the presence of an amorphous structure. A broad peak was observed between 20 and 30° that shows an amorphous character can contribute significantly to the adsorption in terms of forming irregular pores at undefined sites. The formation of scattering humps between 40° and 80° on the 2 $\theta$  axis can indicate the presence of crystal structure that can be attributed to the effect of acid-based pretreatment.

### 3.4 TGA Analysis

Thermal analysis of SBAC shows a broad peak between 25 to 1000 °C showing the thermal characteristics of the sample in terms of mass loss with exposure to temperature change as shown in Fig. 3. SBAC produces a small exothermic peak at 117.7 °C which shows a mass gain of 3.4% which is attributed to a possible oxidation reaction. As the temperature increased from 117.7 to 698.4 °C, the sample began to experience a mass loss of 13.81% due to dehydration or water loss and organic matter degradation of the SBAC. The temperature interval between 698.4 and 1000 °C is associated with the solid residue remaining at the end of the process that contains

**Fig. 1** FTIR spectra for SBAC

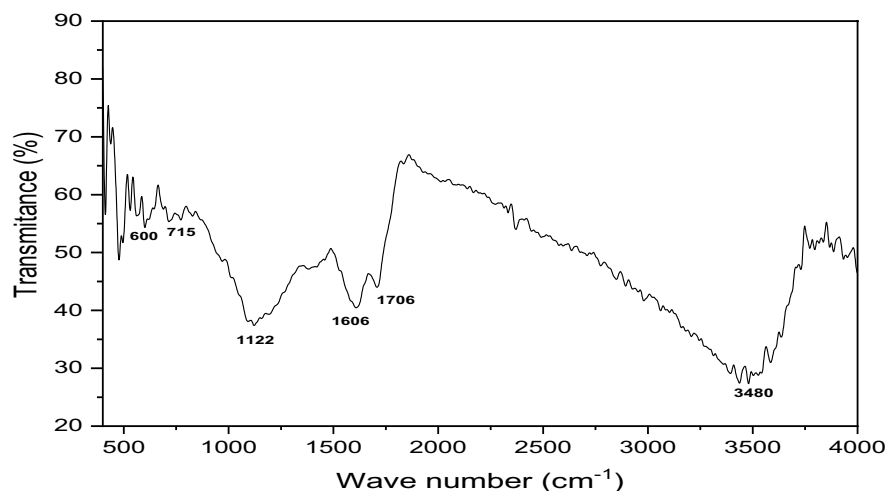
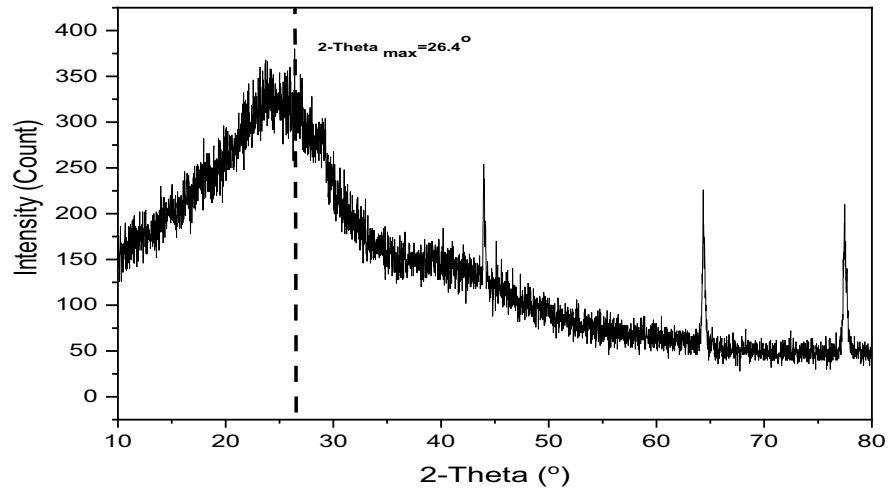


**Fig. 2** XRD pattern for SBAC



ashes and fixed carbons (Van Nam et al., 2019). At this interval, the DTA curve remains constant.

3.5 Effect of Adsorption Parameters

3.5.1 Effect of Adsorbent Dosage

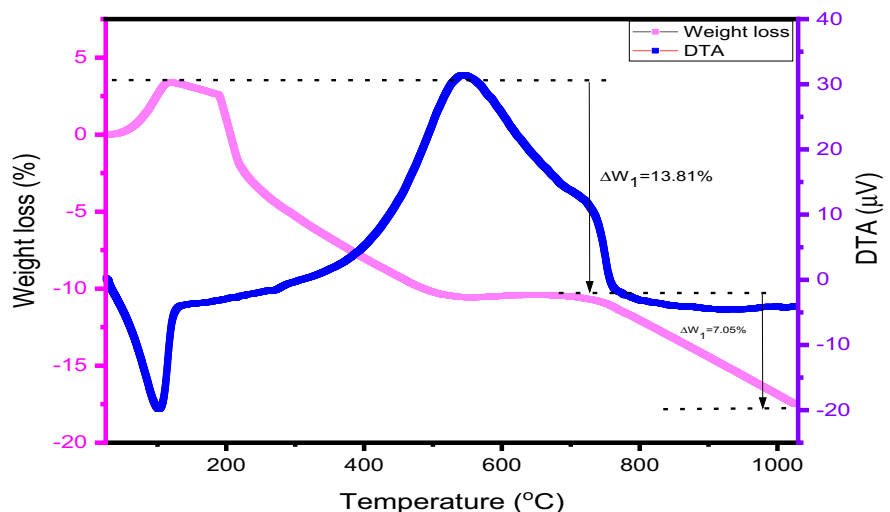
Figure 4a shows the effect of adsorbent dosage on Zn removal efficiency. The highest removal percentage was obtained with doses of 6 gm. The removal efficiency increases with increasing adsorbent dosage. This can be defined, as there are more adsorbents introduced into the system, and the more active sites ready for hosting more adsorbates. Increasing the dosage, the higher the number of available adsorption

sites (Runtti et al., 2016). The maximum efficiency was observed at 6 gm where the graph did not show any sign of turning down.

3.5.2 Effect of Contact Time

As presented in Fig. 4b, the effect of the period of contact on the elimination of Zn (II) ion on batch adsorption in a single cycle is determined in the time intervals of 20, 40, and 60 min. From the profile of the graph, the initial rapid adsorption was observed. The removal efficiency is increasing with time until 40 min which is the time needed to reach the equilibrium. The result shows that from 20 to 40 min, the removal efficiency rose from 75 to 82.4%. Then,

**Fig. 3** Thermogravimetric analysis (TGA) and differential thermal analysis (DTA) for SBAC



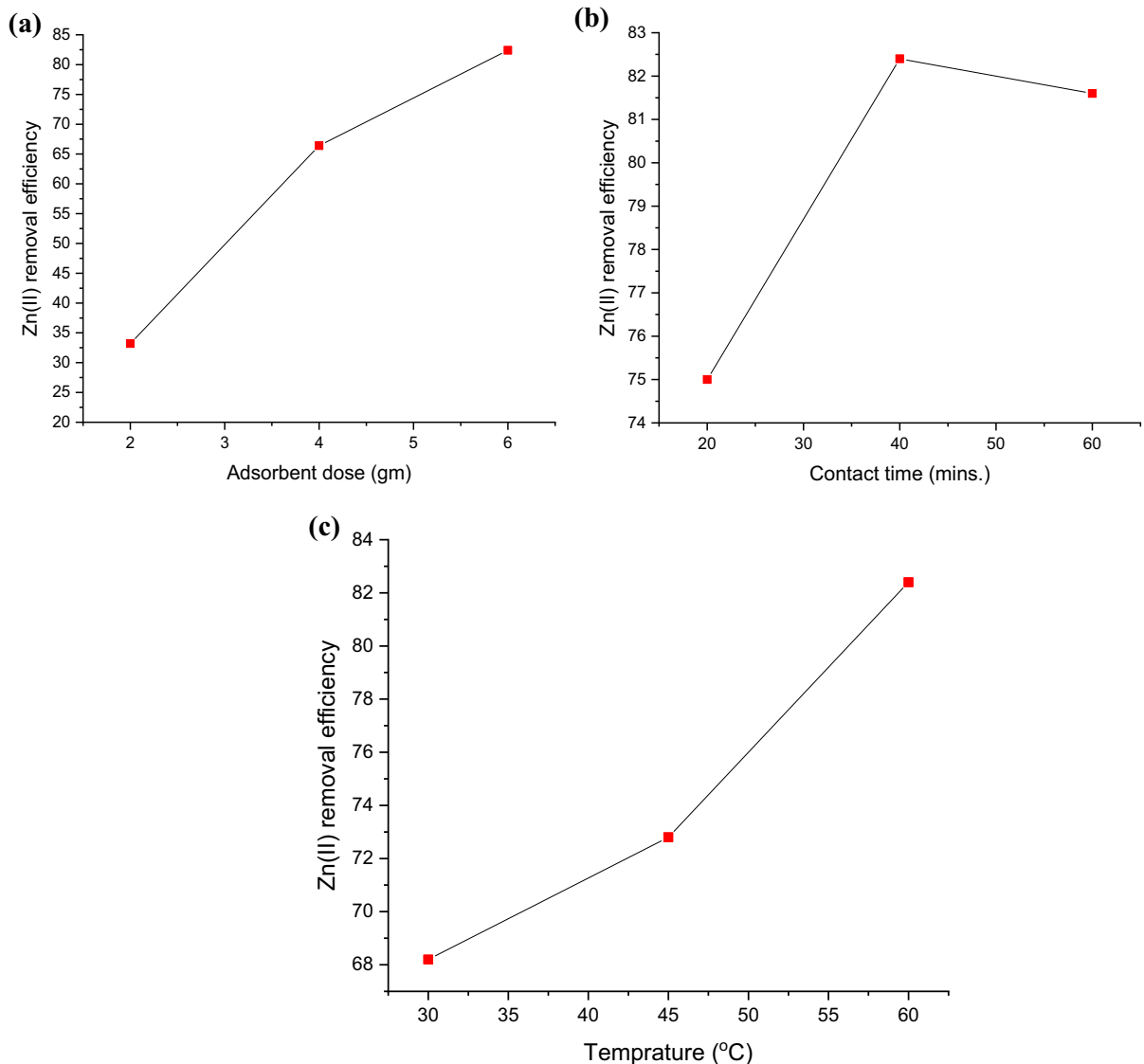


**Fig. 4** Effect of process parameters **a** adsorbent dosage, **b** contact time, and **c** temperature on Zn (II) removal efficiency

when the retention further increased to 60 min, the removal efficiency falls slightly to 81.6%. This phenomenon can be justified through the nature of the adsorbent and its available sorption sites dependent on the time needed to reach the equilibrium (Bhattacharya et al., 2006).

### 3.5.3 Effect of Temperature

The effect of temperature on the removal of Zn in an aqueous solution by SBAC was studied by varying

the temperature between 30 and 60 °C. The data presented in Fig. 4c show that the adsorption of the metal ion by the SBAC increased with a rise in temperature, which is typical for the biosorption of most metal ions from their solution (Ho, 2003; Manju et al., 1998; McKay et al., 1999). The increment in adsorption efficiency with temperature could be one of the indications of the chemisorption process. The chemical reaction might occur between the active functional groups on the surface of SBAC and Zn. In chemisorption, the heat provided turns the activation



energy, and more molecules of adsorbate increase energy and keep energy greater than the activation energy. Therefore, adsorption increases with a temperature rise.

### 3.6 Isotherm Study

In the present study, three isotherms were studied, namely, Langmuir, Freundlich, and Temkin isotherms, and fitted to equilibrium experimental data. The results are shown in Table 3 and the modeled isotherms are plotted in Fig. 5. From the correlation coefficient, the experimental data is best fitted and correlated to Langmuir with  $r^2=0.98758$  which is higher than Freundlich and Temkin with  $r^2=0.98525$  and  $0.98296$ , respectively. The values of  $K_L$  and  $q_m$  were calculated from the slope and intercept from the plot between  $C_e$  and  $C_e/q_e$ . Therefore, the adsorption process of zinc (II) onto SBAC follows the Langmuir isotherm model with high monolayer adsorption. These monolayer adsorption capacities result in a high value of  $q_m$ , i.e.,  $0.42662 \text{ g/g}$  ( $426.62 \text{ mg/g}$ ). Additionally, the significant features of the Langmuir isotherm can be described by the separation factor  $R_L$ , which is calculated by the below equation (Rozada et al., 2007).

$$R_L = \frac{1}{(1 + K_L C_o)} \tag{9}$$

The value of  $R_L$  is classified based on the nature of the adsorption: irreversible ( $RL=0$ ); favorable ( $0 < RL < 1$ ); linear ( $RL=1$ ); and unfavorable ( $RL > 1$ ) (Mohapatra et al., 2009). From the result, the value of  $R_L=0.121515$ , which indicate the process is favorable for the adsorption of Zn (II) using SBAC.

Freundlich isotherm model is the second-best fit in the isotherm study with a regression coefficient  $r^2=0.98525$ . Table 3 shows the Freundlich parameters  $K_F$  and  $1/n$  that were determined from the intercept and slope of the line plot of  $\log q_e$  versus  $\log C_e$ . Since the values of  $1/n$  ( $0.4716$ ), less than 1 reflects the favorability of the adsorption system between the adsorbent SBAC and Zn (II). The adsorption capacity indicating parameters of Freundlich isotherm is  $K_F$  results in a higher magnitude of capacity, i.e.,  $0.56065 \text{ g/g}$  ( $560.65 \text{ mg/g}$ ).

The Temkin isotherm was also fitted to the equilibrium experimental data with  $r^2=0.98296$ .

**Table 3** Isotherm and kinetic model parameters

Isotherm	Parameters	Value
Langmuir	$q_m$ (gm/gm)	0.42662
	$K_L$ (L/gm)	3.442577
	$R_L$	0.121515
	$r^2$	0.98758
Temkin	$B$ (KJ/mol)	26.43
	$K_T$ (L/gm)	12.231
	$r^2$	0.98296
Freundlich	$1/n$	0.4716
	$K_f$ (gm/gm)	0.56065
	$r^2$	0.98525
Kinetics type	Parameters	Value
Pseudo-first-order	$K_1$ ( $\text{min}^{-1}$ )	0.26555893
	$q_e$ (gm/gm)	0.315769
	$r^2$	0.85523
Pseudo-first-order	$K_2$ ( $\text{min}^{-1}$ )	0.1551436
	$q_e$ (gm/gm)	11.7360418
	$r^2$	1
Intraparticle diffusion	$K_{id}$ (gm/gm.mins <sup>0.5</sup> )	0.00134
	$C$	0.14483

The constants  $K_T$  and  $B$  were determined from the plot between  $q_e$  and  $\ln C_e$ . The assumption behind the Temkin isotherm is that due to coverage because of adsorbent-adsorbate interactions, the heat of adsorption of all the molecules in the layer decreases. Therefore, the adsorption is characterized by a homogeneous distribution of the binding energies, up to some maximum binding energy. From the table,  $K_T$  value of  $12.231 \text{ L/gm}$  was obtained which is the equilibrium binding constant for the given binding energy. Another important parameter under Temkin isotherm is the  $b$  value which is related to the heat of sorption. From the result, the calculated heat of sorption for the SBAC to adsorb Zn (II) is  $26.43 \text{ kJ/mol}$ . A positive value of the heat of adsorption indicates that the adsorption is endothermic.

### 3.7 Kinetics Study

To study the likelihood of rate-controlling steps for adsorption, models of pseudo-first-order ( $t$  versus  $\ln(q_e - qt)$ ), pseudo-second-order ( $t$  versus  $(t/qt)$ ), and intraparticle diffusion ( $t^{0.5}$  versus  $qt$ ) are used to fit the experimental data as can be shown from Fig. 5.

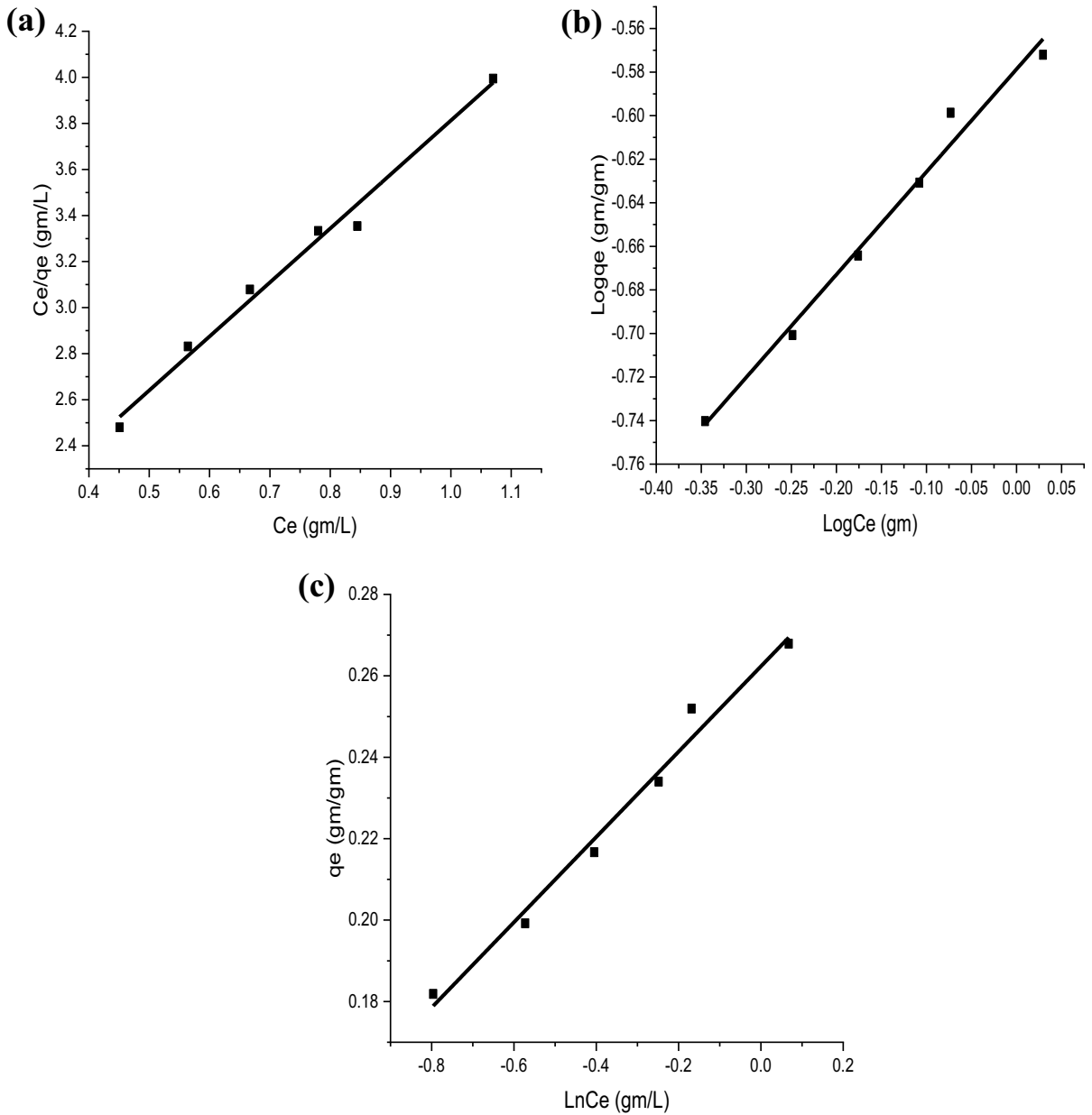


**Fig. 5** Isotherm models **a** Langmuir and **b** Freundlich and **c** Temkin isotherm

To study the mechanism of Zn (II) ion adsorption onto SB surface, the adsorption kinetics was analyzed using pseudo-first-order Lagergren Eq. (9) and pseudo-second-order rate Eq. (10) expressed as follows (Ho & Mckay, 1999):

$$\ln(q_e - q_t) = \ln q_e - \frac{k_1 t}{2.303} \tag{10}$$

$$\frac{t}{q_t} = \frac{1}{k_2 q_e^2} + \frac{t}{q_e} \tag{11}$$

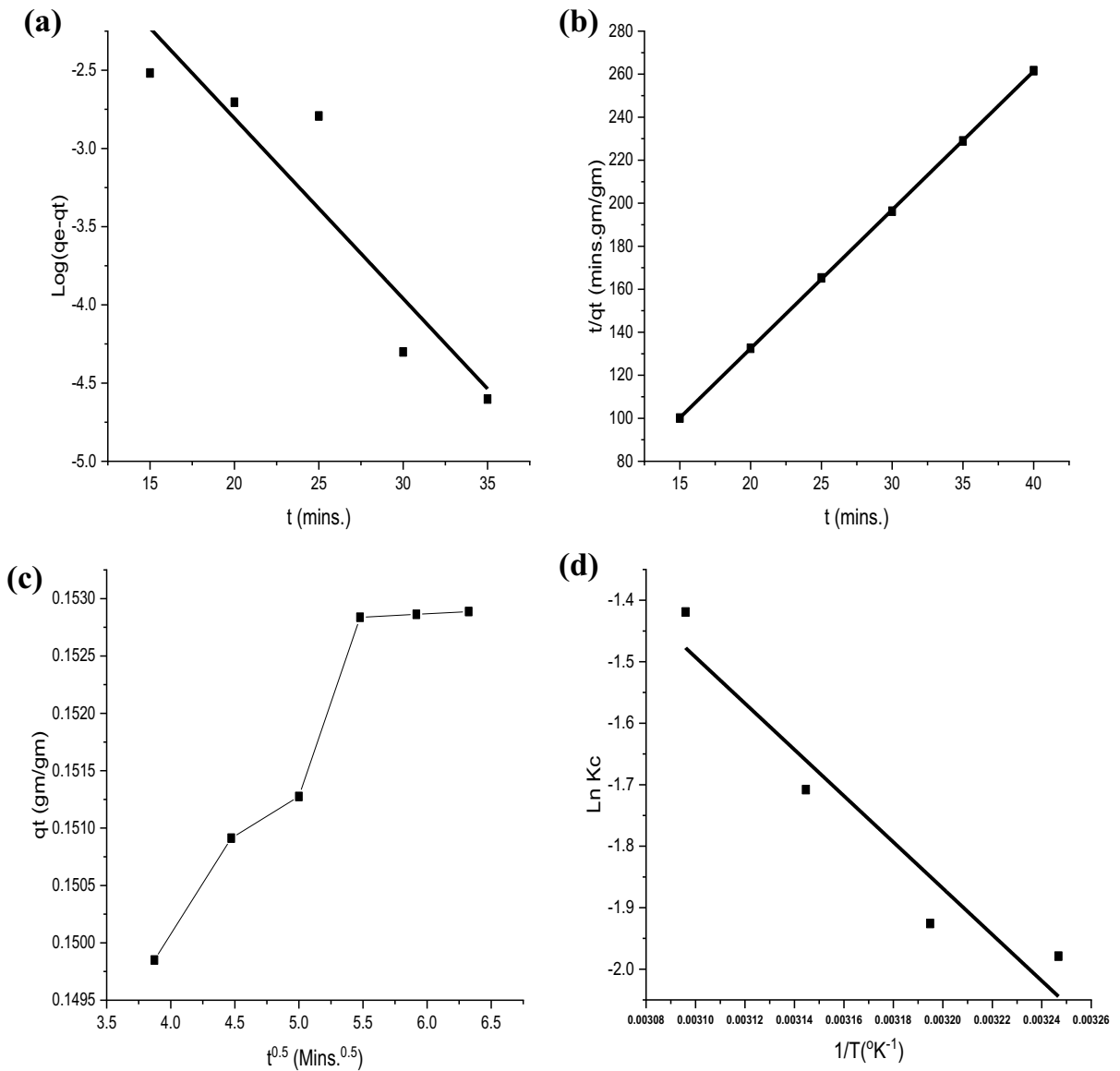


**Fig. 6** Kinetic model and thermodynamics plots, **a** pseudo-second-order, **b** pseudo-second order, **c** intraparticle diffusion, and **d** thermodynamics models

where  $q_t$  is the amount of Zn (II) adsorbed at time  $t$  ( $\text{gm/gm}^{-1}$ ),  $q_e$  is the adsorption capacity at equilibrium ( $\text{gm/gm}$ ),  $k_1$  is the pseudo-first-order rate constant ( $\text{min}^{-1}$ ), and  $k_2$  is the pseudo-first-order rate constant ( $\text{min}^{-1}$ ). The diffusion coefficient for the intraparticle movement of SBAC adsorbent has been calculated at constant by employing rate Eq. (11) according to Weber–Morris model:

$$q_t = K_{id}t^{0.5} + I \tag{12}$$

where  $K_{id}$  is the intraparticle diffusion constant ( $\text{gm/gm min}^{0.5}$ ).

From the table, regression coefficient  $R^2$  and all the calculated parameters are presented. Based on the calculated kinetic model parameters in the table, and the pseudo-second-order model produced by far the best fit

**Table 4** Comparison of the adsorption of Zn (II) ion on SBAC with other adsorbents reported in the literature

Adsorbents	$q_{\max}$ (mg/g)	Reference
Sugarcane bagasse activated carbon	426.64	This study
Modified sugarcane bagasse (MB2)	125	(F. V. Pereira et al., 2009)
Sugarcane cellulose-based adsorbent	363.3	(Wang et al., 2017)
Cassava waste	559.74	(Horsfall & Abia, 2003)
Dried marine green macroalga	128.8	(Ajjabi & Chouba, 2009)
<i>Xanthoceras sorbifolia</i> bunge hull	103.82	(Zhang et al., 2017)
Crab carapace	172.50	(S. Lu et al., 2007)
Chitin shrimp shells	270.27	(Jaafarzadeh et al., 2014)
Chitin crab shells	181.18	(Jaafarzadeh et al., 2014)
Polyethyleneimine	110.2	(Zhan et al., 2018)
Graphene oxide	345	(Sitko et al., 2013)

based on the value of  $R^2$  (1), and these show that the adsorption of Zn (II) on SBAC can be well demonstrated by the pseudo-second-order kinetics model.

### 3.8 Thermodynamics Study

The thermodynamic parameters of adsorption, such as Gibb's free energy ( $\Delta G^\circ$ ), enthalpy ( $\Delta H^\circ$ ), and entropy ( $\Delta S^\circ$ ) changes, were determined from the temperature range between 35 and 50 °C. The following equations (Eqs. (12)–(15)) are used to calculate the thermodynamic parameters:

$$\Delta G^\circ = -RT \ln K_C \quad (13)$$

$$\Delta G^\circ = -RT \ln K_C \quad (14)$$

$$\ln K_C = \frac{\Delta S^\circ}{R} - \frac{\Delta H^\circ}{RT} \quad (15)$$

$$K_C = q_e / C_e \quad (16)$$

where  $R$  is the ideal gas constant ( $8.314 \text{ J mol}^{-1} \text{ K}^{-1}$ ) and  $T$  is the temperature in K.  $K_C$  is the thermodynamic equilibrium constant.

The values of  $\Delta H$  and  $\Delta S$  are determined from the slope and intercept of the plot of  $\ln(K_C)$  versus  $1/T$  as indicated in Fig. 5d. The Gibbs free energy ( $\Delta G$ ) is obtained at a different temperature as summarized in Table 3. The values of  $\Delta G$  as a function of temperature were to be  $-25.9917$  (308 °C),  $-26.4141$  (313 °C),  $-26.8366$  (318 °C), and  $-27.259$  (323 °C) KJ/mol. The decrease of  $\Delta G$  with temperature indicates that the process is spontaneous.

The positive value of  $\Delta H$  (31.26 kJ/mol) indicates the endothermic process. The positive value of  $\Delta S$  ( $84.49 \text{ kJ mol}^{-1} \text{ K}^{-1}$ ) suggests that Zn (II) adsorption onto chemically modified bagasse is an associative mechanism (Mohapatra et al., 2009). A positive value of  $\Delta S$  can also reflect that the adsorption process involves a dissociative mechanism. Such adsorption phenomena are not favorable at high temperatures (Fig. 6).

### 3.9 Comparison with Previously Reported Data for Zinc (II) Adsorption

Table 4 presents a list of different adsorbent materials that have been used to remove zinc (II) ions from aqueous solutions. Comparison among the materials shows that SBAC adsorption capacity ( $q_{\max}$ ) is between the maximum and minimum values reported in the literature. It is worth emphasizing that the use of bioadsorbents such as SBAC is environmentally friendly and it is one of the most powerful adsorbents prepared for industrial wastewater treatment used for the treatment of wastewater contaminated by heavy metals such as zinc (II) ion.—

## 4 Conclusion

In this study, the adsorption of zinc (II) ion onto SBAC was investigated for the dosage of the adsorbent, contact time, and temperature at neutral pH conditions. Equilibrium data agreed better with the Langmuir adsorption isotherm, and it was found to provide the best fit to the experimental data with

a maximum adsorption capacity of 426.64 mg g<sup>-1</sup>. The kinetic model revealed that the experimental data follows the pseudo-second-order model which suggests a chemisorption process. The adsorption process was found to be endothermic and spontaneous and can be explained with the pseudo-second-order type kinetic model. Generally, this study proved that the eco-friendly SBAC adsorbent showed better performance, and the raw material, sugarcane bagasse, is easily available in large quantities, and its treatment method is very economical.

**Data Availability** All data generated or analyzed during this study are included in this published article.

#### Declarations

**Conflict of Interest** The authors declare no competing interest.

#### References

- Ahmad, F., Daud, W. M. A. W., Ahmad, M. A., & Radzi, R. (2013). The effects of acid leaching on porosity and surface functional groups of cocoa (*Theobroma cacao*)-shell based activated carbon. *Chemical Engineering Research and Design*, *91*(6), 1028–1038. <https://doi.org/10.1016/j.cherd.2013.01.003>
- Ajjabi, L. C., & Chouba, L. (2009). Biosorption of Cu<sup>2+</sup> and Zn<sup>2+</sup> from aqueous solutions by dried marine green macroalga *Chaetomorpha linum*. *Journal of Environmental Management*, *90*(11), 3485–3489. <https://doi.org/10.1016/j.jenvman.2009.06.001>
- Ali, I., & Gupta, V. K. (2007). Advances in water treatment by adsorption technology. *Nature Protocols*, *1*(6), 2661–2667. <https://doi.org/10.1038/nprot.2006.370>
- Anoop Krishnan, K., & Anirudhan, T. S. (2002). Removal of mercury(II) from aqueous solutions and chlor-alkali industry effluent by steam activated and sulphurised activated carbons prepared from bagasse pith: Kinetics and equilibrium studies. *Journal of Hazardous Materials*, *92*(2), 161–183. [https://doi.org/10.1016/S0304-3894\(02\)00014-6](https://doi.org/10.1016/S0304-3894(02)00014-6)
- Armbruster, M. H., & Austin, J. B. (1938). The adsorption of gases on plane surfaces of mica. *Journal of the American Chemical Society*, *60*(2), 467–475. <https://doi.org/10.1021/ja01269a066>
- Aslam, M. M., Hassan, I., & Malik, M. (2004). Sand as adsorbent for removal of zinc from industrial effluents. *Electron. J. Environ. Agric. Food Chem*, *3*(6), 792–798.
- ASTM E872-82. (2013). Standard test method for volatile matter in the analysis of particulate wood fuels. *Annual Book of ASTM Standard, American Society for Testing and Materials*.
- Bello, O. S., Adegoke, K. A., & Akinyunni, O. O. (2017). Preparation and characterization of a novel adsorbent from *Moringa oleifera* leaf. *Applied Water Science*, *7*(3), 1295–1305. <https://doi.org/10.1007/s13201-015-0345-4>
- Bhattacharya, A. K., Mandal, S. N., & Das, S. K. (2006). Adsorption of Zn(II) from aqueous solution by using different adsorbents. *Chemical Engineering Journal*, *123*(1–2), 43–51. <https://doi.org/10.1016/j.cej.2006.06.012>
- Capeletti, L. B., & Zimnoch, J. H. (2016). Fourier transform infrared and Raman characterization of silica-based materials. Applications of molecular spectroscopy to current research in the chemical and biological sciences, 1–21. <https://doi.org/10.5772/64477>
- Channiwala, S. A., & Parikh, P. P. (2002). A unified correlation for estimating HHV of solid, liquid and gaseous fuels. *Fuel*, *81*(8), 1051–1063. [https://doi.org/10.1016/S0016-2361\(01\)00131-4](https://doi.org/10.1016/S0016-2361(01)00131-4)
- Demirbas, A. (2008). Heavy metal adsorption onto agro-based waste materials: A review. *Journal of Hazardous Materials*, *157*(2–3), 220–229. <https://doi.org/10.1016/j.jhazmat.2008.01.024>
- Dlapa, P., Bodí, M. B., Mataix-Solera, J., Cerdà, A., & Doerr, S. H. (2013). FT-IR spectroscopy reveals that ash water repellency is highly dependent on ash chemical composition. *CATENA*, *108*, 35–43. <https://doi.org/10.1016/j.catena.2012.02.011>
- Freundlich, H. M. F. (1906). Over the adsorption in solution. *Journal of Physical Chemistry*, *57*(385471), 1100–1107.
- Garca-Pérez, M., Chaala, A., & Roy, C. (2002). Vacuum pyrolysis of sugarcane bagasse. *Journal of Analytical and Applied Pyrolysis*, *65*(2), 111–136. [https://doi.org/10.1016/S0165-2370\(01\)00184-X](https://doi.org/10.1016/S0165-2370(01)00184-X)
- Govindarajan, D., & Jayalakshmi, G. (2011). XRD, FTIR, and SEM studies on calcined sugarcane bagasse ash blended cement. *Archives of Physics Research*, *2*(4), 38–44. Retrieved on June 12, 2022 from <https://scholarsresearchlibrary.com/archive.html>
- Guan, B. T. H., Latif, P. A., & Yap, T. Y. H. (2013). Physical preparation of activated carbon from sugarcane bagasse and corn husk and its physical and chemical characteristics. *International Journal of Engineering Research and Science & Technology*, *2*(3), 1–14.
- Gupta, V. K., & Ali, I. (2000). Utilisation of bagasse fly ash (a sugar industry waste) for the removal of copper and zinc from wastewater. *Separation and Purification Technology*, *18*(2), 131–140. [https://doi.org/10.1016/S1383-5866\(99\)00058-1](https://doi.org/10.1016/S1383-5866(99)00058-1)
- Gupta, V. K., & Ali, I. (2004). Removal of lead and chromium from wastewater using bagasse fly ash - A sugar industry waste. *Journal of Colloid and Interface Science*, *271*(2), 321–328. <https://doi.org/10.1016/j.jcis.2003.11.007>
- Hassan, M. L., & El-Wakil, N. A. (2003). Heavy metal ion removal by amidoximated bagasse. *Journal of Applied Polymer Science*, *87*(4), 666–670. <https://doi.org/10.1002/app.11402>
- Ho, Y. S. (2003). Removal of copper ions from aqueous solution by tree fern. *Water Research*, *37*(10), 2323–2330. [https://doi.org/10.1016/S0043-1354\(03\)00002-2](https://doi.org/10.1016/S0043-1354(03)00002-2)

- Ho, Y. S., & McKay, G. (1999). *Pseudo-second order model for sorption processes*. *34*, 451–465.
- Horsfall, M., & Abia, A. A. (2003). Sorption of cadmium(II) and zinc(II) ions from aqueous solutions by cassava waste biomass (*Manihot sculenta* Cranz). *Water Research*, *37*(20), 4913–4923. <https://doi.org/10.1016/j.watres.2003.08.020>
- Hu, Y., Dong, X., Nan, J., Jin, W., Ren, X., Xu, N., & Lee, Y. M. (2011). Metal-organic framework membranes fabricated via reactive seeding. *Chemical Communications*, *47*(2), 737–739. <https://doi.org/10.1039/c0cc03927f>
- Jaafarzadeh, N., Mengelizadeh, N., Takdastan, A., Heidari-Farsani, M., & Niknam, N. (2014). Adsorption of Zn (II) from aqueous solution by using chitin extraction from crustacean shell. *Journal of Advances in Environmental Health Research*, *2*(2), 110–119.
- Jagaba, A. H., Kutty, S. R. M., Khaw, S. G., Lai, C. L., Isa, M. H., Baloo, L., Lawal, I. M., Abubakar, S., Umaru, I., & Zango, Z. U. (2020). Derived hybrid biosorbent for zinc(II) removal from aqueous solution by continuous-flow activated sludge system. *Journal of Water Process Engineering*, *34*(November 2019), 101152. <https://doi.org/10.1016/j.jwpe.2020.101152>
- Jawad, A. H., Sabar, S., Ishak, M. A. M., Wilson, L. D., Ahmad Norrahma, S. S., Talari, M. K., & Farhan, A. M. (2017). Microwave-assisted preparation of mesoporous-activated carbon from coconut (*Cocos nucifera*) leaf by H<sub>3</sub>PO<sub>4</sub> activation for methylene blue adsorption. *Chemical Engineering Communications*, *204*(10), 1143–1156. <https://doi.org/10.1080/00986445.2017.1347565>
- Jawad, A. H., Razuan, R., Appaturi, J. N., & Wilson, L. D. (2019). Adsorption and mechanism study for methylene blue dye removal with carbonized watermelon (*Citrullus lanatus*) rind prepared via one-step liquid phase H<sub>2</sub>SO<sub>4</sub> activation. *Surfaces and Interfaces*, *16*(April), 76–84. <https://doi.org/10.1016/j.surfin.2019.04.012>
- Jembere, A. L., & Genet, M. B. (2021). Comparative adsorptive performance of adsorbents developed from sugar industrial wastes for the removal of melanoidin pigment from molasses distillery spent wash. *Water Resources and Industry*, *26*, 100165. <https://doi.org/10.1016/j.wri.2021.100165>
- Kadirvelu, K., Thamaraiselvi, K., & Namasivayam, C. (2001). Removal of heavy metals from industrial wastewaters by adsorption onto activated carbon prepared from an agricultural solid waste. *Bioresource Technology*, *76*(1), 63–65. [https://doi.org/10.1016/S0960-8524\(00\)00072-9](https://doi.org/10.1016/S0960-8524(00)00072-9)
- Karnitz, O., Gurgel, L. V. A., de Melo, J. C. P., Botaro, V. R., Melo, T. M. S., de Freitas Gil, R. P., & Gil, L. F. (2007). Adsorption of heavy metal ion from aqueous single metal solution by chemically modified sugarcane bagasse. *Bioresource Technology*, *98*(6), 1291–1297. <https://doi.org/10.1016/j.biortech.2006.05.013>
- Katyal, S., Thambimuthu, K., & Valix, M. (2003). Carbonisation of bagasse in a fixed bed reactor: Influence of process variables on char yield and characteristics. *Renewable Energy*, *28*(5), 713–725. [https://doi.org/10.1016/S0960-1481\(02\)00112-X](https://doi.org/10.1016/S0960-1481(02)00112-X)
- Khalfaoui, A., & Meniai, A. H. (2012). Application of chemically modified orange peels for removal of copper(II) from aqueous solutions. *Theoretical Foundations of Chemical Engineering*, *46*(6), 732–739. <https://doi.org/10.1134/S0040579512060103>
- Kılıç, Z., Atakol, O., Aras, S., Cansaran-Duman, D., & Emregul, E. (2014). Biosorption properties of zinc(II) from aqueous solutions by *Pseudevernia furfuracea* (L.) Zopf. *Journal of the Air and Waste Management Association*, *64*(10), 1112–1121. <https://doi.org/10.1080/10962247.2014.926299>
- Kim, D. Y., Nishiyama, Y., Wada, M., & Kuga, S. (2001). High-yield carbonization of cellulose by sulfuric acid impregnation. *Cellulose*, *8*(1), 29–33. <https://doi.org/10.1023/A:1016621103245>
- Lu, J. J., & Chen, W. H. (2015). Investigation on the ignition and burnout temperatures of bamboo and sugarcane bagasse by thermogravimetric analysis. *Applied Energy*, *160*(2015), 49–57. <https://doi.org/10.1016/j.apenergy.2015.09.026>
- Lu, S., Gibb, S. W., & Cochrane, E. (2007). Effective removal of zinc ions from aqueous solutions using crab carapace biosorbent. *Journal of Hazardous Materials*, *149*(1), 208–217. <https://doi.org/10.1016/j.jhazmat.2007.03.070>
- Mahmoud, M. A. (2014). Adsorption of cadmium onto orange peels: Isotherms, kinetics, and thermodynamics. *Journal of Chromatography & Separation Techniques*, *05*(05). <https://doi.org/10.4172/2157-7064.1000238>
- Maia, L. S., Duizit, L. D., Pinhatio, F. R., & Mulinari, D. R. (2021). Valuation of banana peel waste for producing activated carbon via NaOH and pyrolysis for methylene blue removal. *Carbon Letters*, *31*, 749–762.
- Manju, G. N., Raji, C., & Anirudhan, T. S. (1998). Evaluation of coconut husk carbon for the removal of arsenic from water. *Water Research*, *32*(10), 3062–3070. [https://doi.org/10.1016/S0043-1354\(98\)00068-2](https://doi.org/10.1016/S0043-1354(98)00068-2)
- McKay, G., Ho, Y. S., & Ng, J. C. Y. (1999). Biosorption of copper from waste waters: A review. *Separation and Purification Methods*, *28*(1), 87–125. <https://doi.org/10.1080/03602549909351645>
- Mesa-Perez, J. M., Cortez, L. A. B., Rocha, J. D., Brossard-Perez, L. E., & Olivares-Gómez, E. (2005). Unidimensional heat transfer analysis of elephant grass and sugar cane bagasse slow pyrolysis in a fixed bed reactor. *Fuel Processing Technology*, *86*(5), 565–575. <https://doi.org/10.1016/j.fuproc.2004.05.014>
- Mohapatra, M., Khatun, S., & Anand, S. (2009). Kinetics and thermodynamics of lead (II) adsorption on lateritic nickel ores of Indian origin. *Chemical Engineering Journal*, *155*(1–2), 184–190. <https://doi.org/10.1016/j.cej.2009.07.035>
- Mopoung, S., Moonsri, P., Palas, W., & Khumpai, S. (2015). Characterization and properties of activated carbon prepared from tamarind seeds by KOH activation for Fe(III) adsorption from aqueous solution. *Scientific World Journal* <https://doi.org/10.1155/2015/415961>
- Mulana, F., Mariana, M., Muslim, A., Mohibah, M., & Halim, K. H. K. (2018). Removal of zinc (II) ion from aqueous solution by adsorption onto activated palm midrib bio-sorbent. *IOP Conference Series: Materials Science and Engineering*, *334*(1). <https://doi.org/10.1088/1757-899X/334/1/012027>
- Mulinari, D. R., Voorwald, H. J. C., Cioffi, M. O. H., da Silva, M. L. C. P., & Luz, S. M. (2009). Preparation and

- properties of HDPE/sugarcane bagasse cellulose composites obtained for thermokinetic mixer. *Carbohydrate Polymers*, 75(2), 317–321. <https://doi.org/10.1016/j.carbpol.2008.07.028>
- Nada, A. A. M. A., & Hassan, M. L. (2006). Ion exchange properties of carboxylated bagasse. *Journal of Applied Polymer Science*, 102(2), 1399–1404. <https://doi.org/10.1002/app.24255>
- Van Nam, H., Tam, T. T., & Tho, V. D. S. (2019). Kinetic modeling of thermal decomposition of sugarcane bagasse in the inert gas environment. In *Vietnam Journal of Chemistry* 57(Issue 5) 574–580. <https://doi.org/10.1002/vjch.201900077>
- Pereira, F. V., Gurgel, L. V. A., De Aquino, S.F., & Gil, L. F. (2009). Removal of Zn<sup>2+</sup> from electroplating wastewater using modified wood sawdust and sugarcane bagasse. *Journal of Environmental Engineering*, 135(5), 341–350. [https://doi.org/10.1061/\(ASCE\)0733-9372\(2009\)135:5\(341\)](https://doi.org/10.1061/(ASCE)0733-9372(2009)135:5(341))
- Pereira, F. V., Gurgel, L. V. A., & Gil, L. F. (2010). Removal of Zn<sup>2+</sup> from aqueous single metal solutions and electroplating wastewater with wood sawdust and sugarcane bagasse modified with EDTA dianhydride (EDTAD). *Journal of Hazardous Materials*, 176(1–3), 856–863. <https://doi.org/10.1016/j.jhazmat.2009.11.115>
- Petrov, N., Budinova, T., Razvigorova, M., Ekinci, E., Yardim, F., & Minkova, V. (2000). Preparation and characterization of carbon adsorbents from furfural. *Carbon*, 38(15), 2069–2075. [https://doi.org/10.1016/S0008-6223\(00\)00063-4](https://doi.org/10.1016/S0008-6223(00)00063-4)
- Phuengphai, P., Singjanusong, T., Kheangkhum, N., & Wattanakornsiri, A. (2021). Removal of copper(II) from aqueous solution using chemically modified fruit peels as efficient low-cost biosorbents. *Water Science and Engineering*, 14(4), 286–294. <https://doi.org/10.1016/j.wse.2021.08.003>
- Standard, A. S. T. M. (1755). 01 (2007) Standard test method for ash in biomass. *American Society for Testing and Materials (ASTM) Philadelphia*.
- ASTM, E. 1756 (2015). Standard Test Method for Determination of Total solids in Biomass. *ASTM International, West Conshohocken PA*.
- Qian, C., Li, Q., Zhang, Z., Wang, X., Hu, J., & Cao, W. (2020). Prediction of higher heating values of biochar from proximate and ultimate analysis. *Fuel*, 265, 1128–1132. <https://doi.org/10.1016/j.fuel.2019.116925>
- Rajbhandari, R., Shrestha, L. K., Pokharel, B. P., & Pradhananga, R. R. (2013). Development of nanoporous structure in carbons by chemical activation with zinc chloride. *Journal of Nanoscience and Nanotechnology*, 13(4), 2613–2623. <https://doi.org/10.1166/jnn.2013.7373>
- Rengaraj, S., Yeon, K. H., & Moon, S. H. (2001). Removal of chromium from water and wastewater by ion exchange resins. *Journal of Hazardous Materials*, 87(1–3), 273–287. [https://doi.org/10.1016/S0304-3894\(01\)00291-6](https://doi.org/10.1016/S0304-3894(01)00291-6)
- Rozada, F., Otero, M., García, A. I., & Morán, A. (2007). Application in fixed-bed systems of adsorbents obtained from sewage sludge and discarded tyres. *Dyes and Pigments*, 72(1), 47–56. <https://doi.org/10.1016/j.dyepig.2005.07.016>
- Runtti, H., Tuomikoski, S., Kangas, T., Kuokkanen, T., Rämö, J., & Lassi, U. (2016). Sulphate removal from water by carbon residue from biomass gasification: Effect of chemical modification methods on sulphate removal efficiency. *BioResources*, 11(2), 3136–3152. <https://doi.org/10.15376/biores.11.2.3136-3152>
- Safari, E., Rahemi, N., Kahforoushan, D., & Allahyari, S. (2019). Copper adsorptive removal from aqueous solution by orange peel residue carbon nanoparticles synthesized by combustion method using response surface methodology. *Journal of Environmental Chemical Engineering*, 7, 102847. <https://doi.org/10.1016/j.jece.2018.102847>
- Salihi, I. (2015). InCIEC 2014. *InCIEC 2014, June 2017*. <https://doi.org/10.1007/978-981-287-290-6>
- Šćiban, M., Radetić, B., Kevrešan, Ž., & Klačnja, M. (2007). Adsorption of heavy metals from electroplating wastewater by wood sawdust. *Bioresource Technology*, 98(2), 402–409. <https://doi.org/10.1016/j.biortech.2005.12.014>
- Senthilkumar, R., Vijayaraghavan, K., Thilakavathi, M., Iyer, P. V. R., & Velan, M. (2006). Seaweeds for the remediation of wastewaters contaminated with zinc(II) ions. *Journal of Hazardous Materials*, 136(3), 791–799. <https://doi.org/10.1016/j.jhazmat.2006.01.014>
- Sia, G. B., Vernasqui, L. G., Consolin-Filho, N., Gonçalves, M. S., & Medeiros, F. V. da S. (2022). Zinc adsorption from aqueous solution on biosorbent from urban pruning waste. *Environmental Technology (United Kingdom)*, 43(5), 728–736. <https://doi.org/10.1080/09593330.2020.1803418>
- Sitko, R., Turek, E., Zawisza, B., Malicka, E., Talik, E., Heimann, J., Gagor, A., Feist, B., & Wrzalik, R. (2013). Adsorption of divalent metal ions from aqueous solutions using graphene oxide. *Dalton Transactions*, 42(16), 5682–5689. <https://doi.org/10.1039/c3dt33097d>
- Srivastava, V. C., Mall, I. D., & Mishra, I. M. (2006). Equilibrium modelling of single and binary adsorption of cadmium and nickel onto bagasse fly ash. *Chemical Engineering Journal*, 117(1), 79–91. <https://doi.org/10.1016/j.cej.2005.11.021>
- Tempkin, M. J., & Pyzhev, V. (1940). Recent modifications to Langmuir isotherms. *Acta Physiochim. USSR*, 12, 217–222.
- Tsai, W. T., Lee, M. K., & Chang, Y. M. (2006). Fast pyrolysis of rice straw, sugarcane bagasse and coconut shell in an induction-heating reactor. *Journal of Analytical and Applied Pyrolysis*, 76(1–2), 230–237. <https://doi.org/10.1016/j.jaap.2005.11.007>
- Wan Ngah, W. S., & Hanafiah, M. A. K. M. (2008). Removal of heavy metal ions from wastewater by chemically modified plant wastes as adsorbents: A review. *Bioresource Technology*, 99(10), 3935–3948. <https://doi.org/10.1016/j.biortech.2007.06.011>
- Wang, F., Pan, Y., Cai, P., Guo, T., & Xiao, H. (2017). Single and binary adsorption of heavy metal ions from aqueous solutions using sugarcane cellulose-based adsorbent. *Bioresource Technology*, 241, 482–490. <https://doi.org/10.1016/j.biortech.2017.05.162>

- Wuana, R. A., & Okieimen, F. E. (2011). Heavy Metals in Contaminated Soils: A Review of Sources, Chemistry, Risks and Best Available Strategies for Remediation. *ISRN Ecology*, 2011, 1–20. <https://doi.org/10.5402/2011/402647>
- Yılmaz, O., & Tugrul, N. (2022). Zinc adsorption from aqueous solution using lemon, orange, watermelon, melon, pineapple, and banana rinds. *Water Practice and Technology*, 17(1), 318–328. <https://doi.org/10.2166/wpt.2021.102>
- Zhan, W., Xu, C., Qian, G., Huang, G., Tang, X., & Lin, B. (2018). Adsorption of Cu(ii), Zn(ii), and Pb(ii) from aqueous single and binary metal solutions by regenerated cellulose and sodium alginate chemically modified with polyethyleneimine. *RSC Advances*, 8(33), 18723–18733. <https://doi.org/10.1039/c8ra02055h>
- Zhang, X., Hao, Y., Wang, X., & Chen, Z. (2017). Rapid removal of zinc(II) from aqueous solutions using a mesoporous activated carbon prepared from agricultural waste. *Materials*, 10(9). <https://doi.org/10.3390/ma10091002>

**Publisher's Note** Springer Nature remains neutral with regard to jurisdictional claims in published maps and institutional affiliations.